JOURNAL OF MATERIALS SCIENCE 21 (1986) 781–787

Infrared optical constants for CO_2 laser waveguide materials

C. A. WORRELL
ERA Technology Ltd, Cleeve Road, Leatherhead, Surrey KT22 7SA, UK

The infrared optical constants of a number of commercially available glasses and ceramics have been determined by Kramers–Krönig analyses of the reflectance spectra of the materials at near normal incidence. The data derived, the refractive index n, and extinction coefficient K, have been further analysed to provide an assessment of these materials as hollow waveguides at mid-infrared frequencies. The results demonstrate that the frequency dependence of waveguide transmission is a feature of anomalous dispersion. Furthermore, in the case of beryllia and alumina ceramics, the high transmissions predicted in straight guide at 10.6 μm can be attributed to the low refractive indices measured for these materials. Some experimental data are presented which substantiate the frequency characteristics of the predicted waveguide transmission.

1. Introduction

A developing interest in the optical properties of materials at infrared frequencies (5 to 55 μm) has been recently stimulated by the commercialization of the comparatively cheap and compact high power CO_2 gas laser operating at 10.6 μm. In medical, military and industrial engineering applications, this laser has generated a requirement for the characterization of materials in terms of their absorbance, reflectance and transmittance properties. In this respect, the bulk optical properties, refractive index, n, and extinction coefficient, K, will completely define such interactions, and are the properties of particular interest in the development and assessment of materials for laser waveguides either in laser tubes or delivery systems. Whereas such data at mid-infrared frequencies is available for metals and some single crystals, very little is known on the absorption and dispersion properties at these wavelengths for commercially available glasses and ceramics.

In the development of CO_2 waveguides, a number of different materials and designs have been proposed. The constructions are essentially of two types, these being hollow and solid core. The hollow core fibres or waveguides can be further classified as metal [1, 2], metal/dielectric coated [3, 4], hollow glass [5, 6] or ceramic. For the solid core fibres, interest has mainly centred on the wide band infrared transmitting materials such as the crystalline alkali halides [7], and the halides of silver [8] and thallium, e.g. KRS5 [9, 10]. Whereas fibres from these materials have been fabricated with low losses, problems have been encountered with mechanical failure on flexing, together with environmental and photodegradation. With the exception of hollow glass and ceramic waveguides much of the development has concerned fibre fabrication of materials of known optical properties.

A hollow fibre or waveguide, particularly that based on glass, presents an attractive alternative to the solid core type, since the fibre core is air and is essentially loss free. However, a disadvantage experienced with this type of waveguide is the loss encountered on bending. Recent advances suggest this may be overcome using a dielectric coating on the inner reflecting surface of a metal guide [4]. An approach recently proposed [5] concerns a hollow glass fibre in which the glass or cladding material has a refractive index of less than unity at 10.6 μm and can thus, in principle, provide a total internal reflecting condition. A refractive index of less than unity follows from the anomalous dispersion effects exhibited by many crystalline and vitreous inorganic materials in the region of 10.6 μm.

Clearly waveguide propagation and losses ultimately depend on the optical properties, refractive index, n, and extinction coefficient, K, of the materials employed. Such data will become of increasing importance as novel materials and waveguide designs are developed. Although this information is required specifically at 10.6 μm, spectral data is necessary to provide a basis for the formulation of novel materials.

In the present work the optical constants, n and K, of commercial materials used as waveguides in CO_2 laser applications are reported. The glasses studied are silica based, these being clear fused silica (i.e. vitreous silica), Pyrex and soda-lime. For the ceramic materials, beryllia and alumina have been studied, and these include samples manufactured by different processing and with compositional changes.

2. Experimental details

The method employed for the determination of n and K is that based on a Kramers–Krönig analysis of the measured reflectance spectrum at near normal incidence. Under these conditions the equations relating n and K to R, which measures the intensity of reflectance, are as follows:

0022–2461/86 $03.00 + .12

TABLE I

Sample	Composition (wt %)	Density ($kg\,m^{-3} \times 10^{-3}$)
D975*	97.5 Al_2O_3	3.78
D995*	99.5 Al_2O_3	3.87
D999*	99.9 Al_2O_3	3.95
Hot pressed Al_2O_3†	99.5 Al_2O_3	3.98
BeO (1)‡	99.5 BeO	2.86
BeO (2)‡	99.8 BeO	~2.93
Soda-lime glass	72% SiO_2, 14% Na_2O 7.1% CaO, 4% MgO, 1.9% Al_2O_3	
Pyrex (Corning 7740)	80.6% SiO_2, 12.6% B_2O_3, 4.2% Na_2O, 2.2% Al_2O_3	
Clear fused silica (Heraeus)	~100% SiO_2	

*Supplied by Anderman and Ryder.
†Fabricated at ERA Technology Ltd.
‡Supplied by Consolidated Beryllium.

$$n = \frac{1 - R}{1 + R - 2R^{\frac{1}{2}} \cos\theta} \quad (1)$$

$$K = \frac{2R^{\frac{1}{2}} \sin\theta}{1 + R - 2R^{\frac{1}{2}} \cos\theta} \quad (2)$$

In the above, θ is defined as the change in the phase angle between the reflected and incident beams, and if R and θ are known at each frequency, ν_a, the optical constants n and K can be calculated. The reflectance intensity coefficient, R, is measureable, but an indirect method is necessary for the evaluation of θ. This involves the application of the Kramers–Krönig integral transform which relates θ to R at a frequency ν_a as in

$$\theta(\nu_a) = \frac{-2\nu_a}{\pi} \int_0^\infty \frac{\ln r(\nu) - \ln r(\nu_a) d\nu}{(\nu^2 - \nu_a^2)} \quad (3)$$

A number of computational procedures have been developed for the integration of equations of the type in Equation 3; however, the procedure adopted in this work is that described in more detail by Gaskell and Johnson [11].

The materials selected for the present investigation were supplied by a number of manufacturers, and are identified in Table I. The surface finish of all glass samples were as-cast from the melt, the hot pressed alumina was as-fired, whereas the remaining ceramics were ground and polished to 0.25 μm grit size diamond paste. The reflectance measurements were undertaken using a Perkin Elmer 983G grating dispersive spectrophotometer, and subsequent data processing with a Data Station 3600. The wavelength range studied was 2000 to 180 cm^{-1} (5 to 55 μm) with a resolution nominally 3 to 8 cm^{-1} in the range 2000 to 300 cm^{-1} and 8 to 13 cm^{-1} in the range 360 to 180 cm^{-1}. The ordinate precision was approximately 0.1% R. Reflectance measurements were undertaken using a relative reflectometer accessory which provided an average angle of incidence of 6.5°. Each spectrum was recorded by a direct substitution method with reference to a calibrated front aluminized mirror

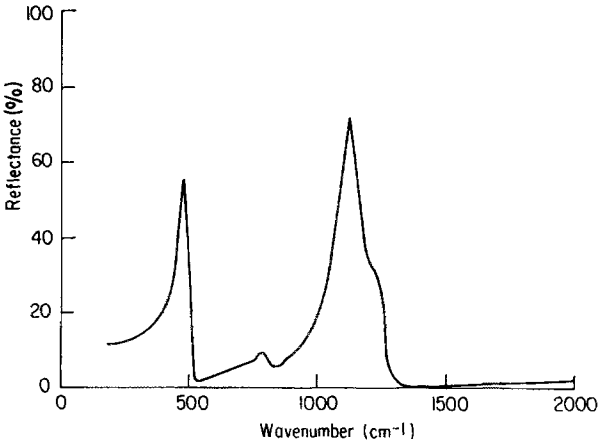

Figure 1 Infrared reflectance spectrum for clear fused silica, SiO_2.

[12]. Both the mirror and sample reflectance were corrected for background scattered and reflected radiation using spectral subtraction, and the reflectance of each sample was then computed by spectral difference. For each spectrum reported herein, the average of three such measurements described above is presented. Subsequent processing of this data to provide n and K then followed using the Kramers–Krönig analysis described by Gaskell and Johnson [11]. This method requires specular reflectance data at frequencies defined by the ratio 1.005. Thus, in the range 2000 to 180 cm^{-1}, a total of 482 reflectance data points were necessary to cover the spectral range of interest.

3. Results and discussion

3.1. Infrared reflectance data

An assessment of the precision and accuracy of the data presented has been made. As described above, three measurements of specular reflectance were undertaken for each sample which in turn provided three sets of n and K data. Whereas the mean of this data is that presented, the difference between individual sets with this mean provides a measurement of precision. The data processed in this way indicated that the reproducibility in reflectance coefficient R was $\pm 2 \times 10^{-3}$, and for n nd K the precision was generally better than $\pm 2 \times 10^{-2}$.

The optical properties for vitreous silica presented in Figs. 1 and 2 (clear fused silica) provide a useful

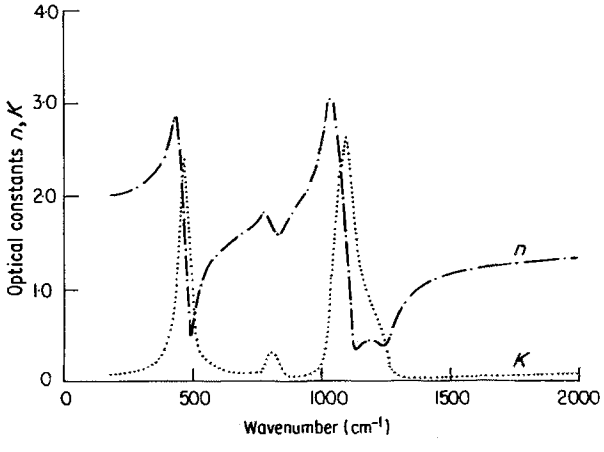

Figure 2 Optical constants, refractive index, n, and extinction coefficient, K, for clear fused silica, SiO_2.

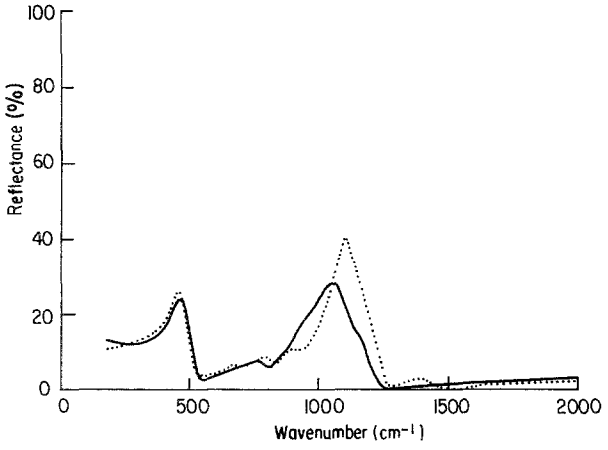

Figure 3 Infrared reflectance spectra: (a) —soda lime glass, (b) ···· Pyrex.

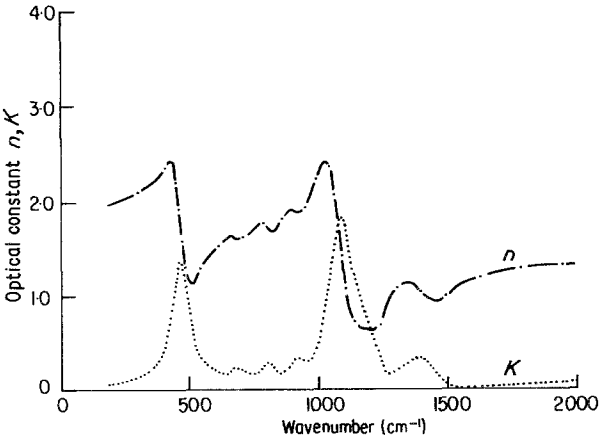

Figure 5 Optical constants, refractive index, n, and extinction coefficient, K, for Pyrex.

comparison with existing published data. Although different materials of manufacture and grade will reflect differences in the corresponding optical properties, a comparison of the results presented herein can be made with those given by Gaskell and Johnson [11]. The Kramers–Krönig transform applied follows from their work, and thus only small changes due to different samples are expected. Although evidence of the very weak bands at ~ 920 and $\sim 600\,cm^{-1}$ are not conclusive for the vitreous silica measured in this work (see Fig. 1), a comparison of oscillator frequencies, refractive index profiles and integrated band intensities shows a good measure of correlation.

The specular reflectance data measured for the remaining glasses are presented in Fig. 3. Detailed vibrational spectroscopic assignments of these spectra are not within the scope of this work since these have been mainly covered elsewhere. However some general points are noteworthy. For vitreous silica attempted assignments of vibrational modes based on idealized structural units have met with a measure of success; nevertheless the interpretations can be ambiguous. However, it is generally accepted that the strong reflectance band at $1124\,cm^{-1}$ is due to an Si–O–Si bond stretching vibration involving primarily oxygen atoms, and the reflectance band at $480\,cm^{-1}$ is considered to involve angular deformation modes involving primarily displacements of the oxygen atoms.

The soda-lime and Pyrex glass spectra in Fig. 3 illustrate the band broadening effect on the high frequency Si–O–Si bond stretch. This is a feature normally associated with the additions of divalent and monovalent cations such as Na^+ and Ca^{2+}. Their presence usually modifies the three-dimensional continuity of the silicon oxygen network with the formation of $Si–O^-$ type bonds. The vibrational frequency for this type of bond is displaced to lower frequencies, i.e. towards $900\,cm^{-1}$, giving the band broadening effect. In the case of Pyrex the additions of boron oxide and alumina almost certainly account for the presence of weak bands at approximately $1380\,cm^{-1}$ and $670\,cm^{-1}$ respectively (see Figs. 3 and 5).

The reflectance spectra for the alumina ceramic materials are presented in Figs. 6 and 7, and for the beryllia ceramics in Fig. 9. A preliminary search of the literature has not revealed any comparative data on n and K for beryllia and alumina ceramics. Single crystal measurements on alumina (i.e. corundum and sapphire) have been made by some authors [13, 14] and similarly for beryllia [15]. The reflectance spectrum of the hot pressed alumina displayed in Fig. 6 shows some similarity with the published data for sapphire. However, a notable difference is the presence of a weak band at approximately $500\,cm^{-1}$ which is observed in all alumina samples studied in this work. According to Barker [13] and Zanzucchi *et al.* [14], the reflectance band at $\sim 600\,cm^{-1}$ for single crystal

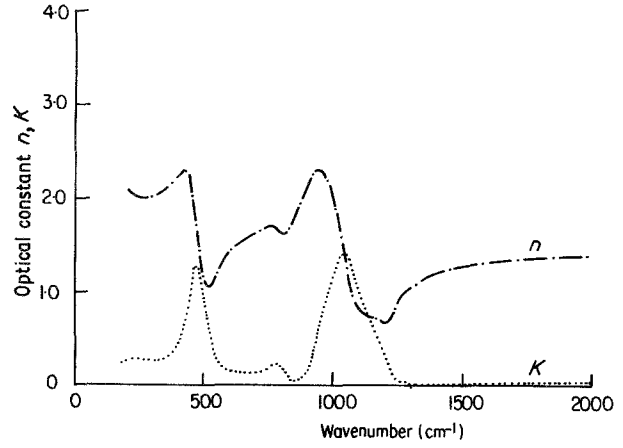

Figure 4 Optical constants, refractive index, n, and extinction coefficient, K, for soda-lime glass.

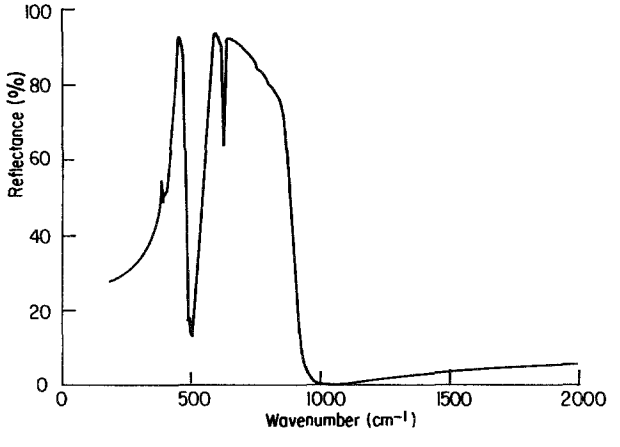

Figure 6 Infrared reflectance spectrum for hot pressed alumina, 99.9% Al_2O_3.

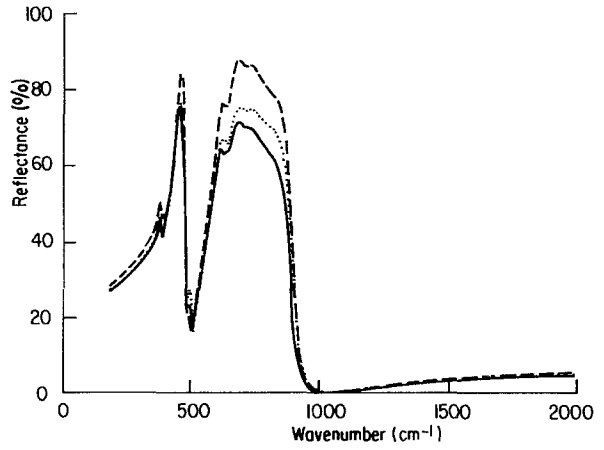

Figure 7 Infrared reflectance spectra for alumina: (a) —99.9% Al_2O_3, (b) ····99.5% Al_2O_3, (c) —97.5% Al_2O_3.

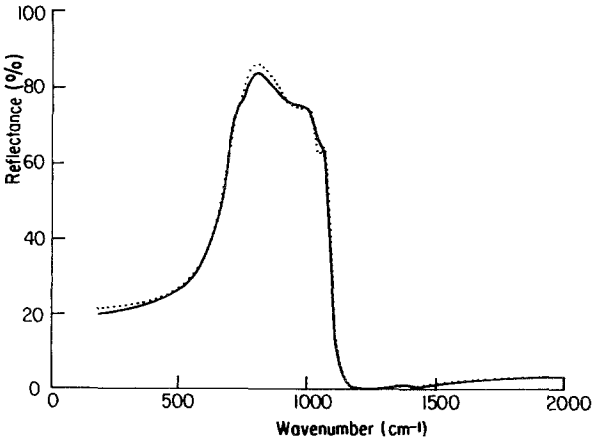

Figure 9 Infrared reflectance spectra for beryllia, (a) —BeO (1), (b) ···· BeO (2).

alumina is sensitive to surface strain effects induced by mechanical polishing. An increase in intensity and resolution is noted for this band in the hot pressed alumina when compared to the shoulder that appears at approximately the same frequency for the alumina ceramics studied. Although the hot pressed alumina presented an as-fired mirror finish surface and was not mechanically polished, it is more likely that the reflectance spectrum recorded for this material is indicative of a higher degree of crystallinity and orientation of the ceramic microstructure. A comparison of densities for the alumina ceramics, as given in Table I, shows quite clearly a correlation of this data with the reflectance intensity coefficients measured, i.e. an increase in reflectance follows an increase in density.

Although a number of different samples of beryllia ceramics were measured, they were all of similar density, and thus the reflectance intensity coefficients did not show the extent of variations measured for the alumina ceramics. The spectra presented in Fig. 9 highlight the main differences observed. A comparison of these measurements with those reported for single crystal beryllia shows a similar Reststrahlen band in the region 1200 to 600 cm^{-1}. However, in the case of the ceramic materials, the maximum in reflectance around 800 cm^{-1} is less than that reported for the single crystal. Also differences in band profile are noted with the appearance of shoulder bands at approximately 1070 and 710 cm^{-1} in the ceramic materials, together with a weak band at ~1390 cm^{-1}.

A reduction in the reflection amplitude of the Reststrahlen band for the ceramic materials can be attributed to a lower density and thus revealed porosity at the reflecting surface, together with the polycrystalline nature of the material and the degree of crystallinity.

3.2. Optical properties and waveguide/frequency transmission

The reflectance data for all materials reported has been transformed as described above to provide refractive index and extinction coefficient profiles over the frequency range studied. For fused silica, Pyrex and soda-lime glasses these are presented in Figs. 2, 4 and 5. For the ceramic materials (i.e. hot pressed alumina and beryllia) the results are given in Figs. 8 and 10, respectively. To assess the suitability of these materials as hollow waveguides for the CO_2 laser, the optical constant data was further processed to provide an estimation of transmission of each material fabricated into a straight hollow waveguide. The model used is depicted in Fig. 11 and the method follows the ray optic calculations of Hidaka *et al.* [5], in which the reflection losses per metre length of guide are calculated and then transformed into transmission per metre, i.e. $T\%\ m^{-1}$. The model described is only a rough approximation since a two dimensional analysis has been invoked, and the lowest loss mode for circular guide (i.e. HE_{11}) has been approximated to by random polarization. However, the method should prove

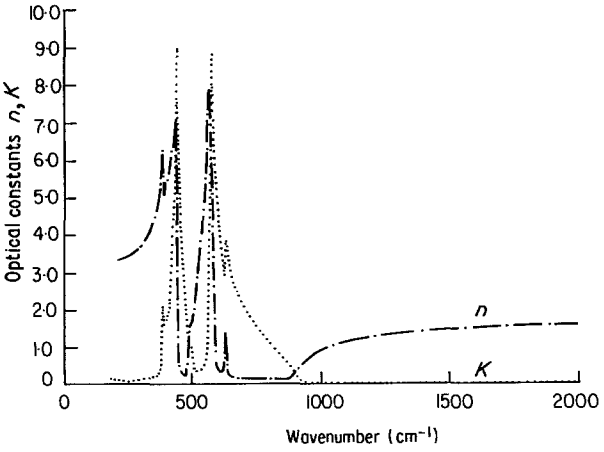

Figure 8 Optical constants, refractive index, n, and extinction coefficient, K, for hot pressed alumina, 99.9% Al_2O_3.

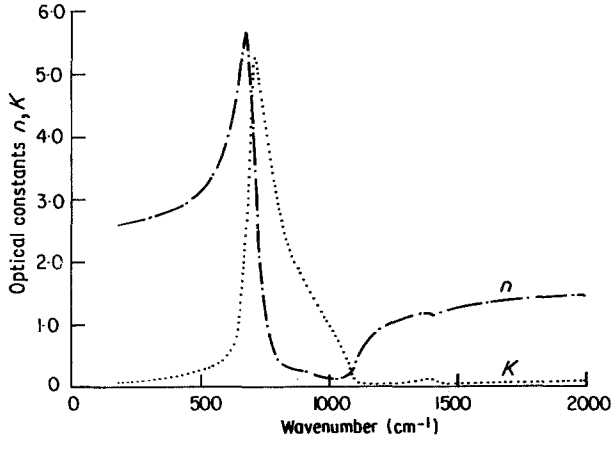

Figure 10 Optical constants, refractive index, n, and extinction coefficient, K, for BeO (1), beryllia.

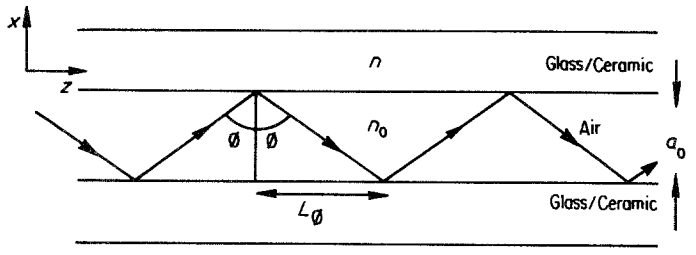

Figure 11 Model for hollow core glass/ceramic waveguide for calculation of waveguide transmission loss.

useful in ranking materials in order of relative 'merit', and is particularly convenient for calculating the frequency dependence of predicted transmission.

For the model depicted in Fig. 11, light propagates along the XZ plane. The core diameter is a_0 with a refractive index n_0 (in this case air, thus $n_0 = 1$). The glass has a refractive index n as expressed in the complex refractive index $\hat{N} = n - iK$, wherein K is the extinction coefficient. The incidence angle at the glass–air interface is ϕ, and the period of reflection is L_ϕ. For the lowest loss mode, and according to Hidaka *et al.* [5], the angle of incidence is thus

$$\phi = \cos^{-1}\left(\frac{\lambda_0}{2a_0}\right) \tag{3}$$

wherein λ_0 is the wavelength in vacuo.

The electric field reflection amplitudes perpendicular and parallel to the plane of incidence are given in the following Fresnel equations

$$r_\perp = \frac{a^2 + b^2 - 2a\cos\phi + \cos^2\phi}{a^2 + b^2 + 2a\cos\phi + \cos^2\phi} \tag{4}$$

$$r_\parallel = r_\perp \frac{a^2 + b^2 - 2a\sin\phi\tan\phi + \sin^2\phi\tan^2\phi}{a^2 + b^2 + 2a\sin\phi\tan\phi + \sin^2\phi\tan^2\phi} \tag{5}$$

wherein

$$2a^2 = [(n^2 - K^2 - \sin^2\phi)^2 + 4n^2K^2]^{\frac{1}{2}} + [(n^2 - K^2) - \sin^2\phi] \tag{6}$$

$$2b^2 = [(n^2 - K^2 - \sin^2\phi)^2 + 4n^2K^2]^{\frac{1}{2}} - [(n^2 - K^2) - \sin^2\phi] \tag{7}$$

Assuming random polarization in the fibre core, the reflection amplitude per reflection is then given by

$$r(\phi) = \frac{1}{2}[r_\parallel + r_\perp] \tag{8}$$

The percentage transmittance T per unit length then becomes

$$T = 100[R(\phi)]^{\frac{1}{L_\phi}} \tag{9}$$

where R is the reflectance intensity coefficient $= r^2$, and $1/L_\phi = 1/a_0 \tan\phi$.

By substituting values for λ_0 and a_0 into Equation 3 to give incidence angle ϕ, followed by n, K and ϕ into Equations 4 to 8 to give reflectance coefficient R, the waveguide loss can then be estimated using Equation 9. Repeating this calculation for each wavelength at which n and K have been experimentally derived provides an estimate of waveguide transmission and its variation with frequency. The optical constant data reported for the materials described in the work have been analysed in this way, and the bore size selected was 0.5 mm. The transmissions per metre against frequency data are presented in Figs. 12 to 16.

The ceramic materials indicate a high transmission window around 900 to 1000 cm^{-1}, whereas the glasses illustrate a similar effect at shorter wavelengths, i.e. around 1100 to 1200 cm^{-1}. The predicted transmission loss (dB m^{-1}) is at 10.6 μm (943 cm^{-1}) for each material presented in Table II. This data suggests that for the materials studied, the beryllia and hot pressed alumina ceramics will give the highest transmission at CO_2 laser wavelengths, and furthermore, in the case of alumina, the results demonstrate that an increase in transmission at 10.6 μm follows an increase in ceramic density. The minor differences in predicted transmission for the two beryllia ceramics reflect the small differences in density of these materials. The high transmission for the ceramics compared to the glasses

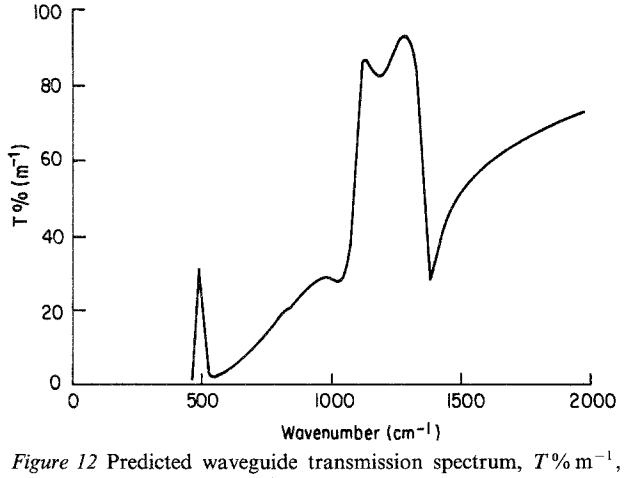

Figure 12 Predicted waveguide transmission spectrum, $T\%\,m^{-1}$, for clear fused silica, SiO_2.

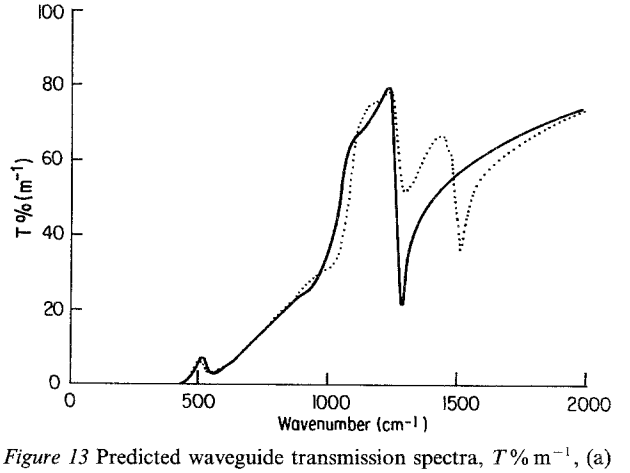

Figure 13 Predicted waveguide transmission spectra, $T\%\,m^{-1}$, (a) —soda-lime glass, (b) ···· Pyrex.

TABLE II

Sample	Predicted transmission loss at 10.6 μm (dB m^{-1})
D975	1.33
D995	0.69
D999	0.76
Hot pressed Al_2O_3	0.52
BeO (1)	0.56
BeO (2)	0.55
Soda-lime	5.73
Pyrex	5.41
Clear fused silica	5.06

are borne out in their application as guides in CO_2 waveguide lasers. The data presented in this work clearly demonstrates that this high transmission is due to the anomalous dispersion effects of these materials around 10.6 μm. Thus, the combined effects of a decreasing refractive index, and less than unity, together with a reducing extinction coefficient leads to an increase in transmission for a given frequency.

To substantiate further the theoretical transmission frequency characteristics discussed above, the materials in the form of small bore diameter tubes were investigated spectroscopically. Short lengths of approximately 2 to 3 cm and bore sizes 1 to 2 mm were supported in an iris diaphragm and positioned in the sample beam of the infrared spectrophotometer. The radiation detected was that which passed down the fibre, and thus mainly reflected from the internal surface. The transmission for each tube was of the order of 2 to 10%, but was adequate to provide spectral information in the range 2000 to 300 cm^{-1}. A sample of each material, with the exception of beryllia, was scanned in this range, and the spectra obtained are presented in Fig. 17. Although the tubes were not fabricated from identical materials as those used in the optical constant determinations, the spectroscopic transmission characteristics show a very good correlation between theory and experiment. The experimental transmissions are depicted on an arbitrary scale; nevertheless, the windows observed for each material occur at similar frequencies and are of similar profile to those given in the theoretical curves derived from the optical constant data.

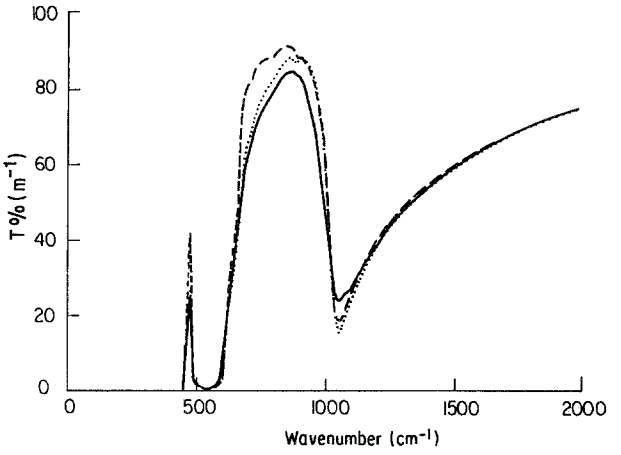

Figure 15 Predicted waveguide transmission spectra, $T\%\,m^{-1}$, for alumina, (a) —D999 alumina, (b) ···· D995 alumina, (c) —D975 alumina.

4. Conclusions

The infrared optical properties of a number of commercially available glasses and ceramics have been derived from their normal incidence reflectance spectra. The optical constant data have been analysed to provide an assessment of these materials as hollow waveguides at mid-infrared frequencies. For the commercial materials studied, the results indicate that beryllia ceramics will give the highest transmission in straight guide at 10.6 μm (i.e. 943 cm^{-1}). However, this data also indicates that similar transmissions could be achieved with alumina ceramics of high densification. The optical constant data demonstrates that the frequency dependence of waveguide transmission is a feature of anomalous dispersion. Furthermore, the increase in transmission for beryllia and alumina around the CO_2 lasing frequencies can be attributed to the low refractive index (i.e. less than unity) measured for these materials.

Clearly the development of hollow flexible waveguides based on the ceramic materials studied herein, would impose considerable fabrication problems. However, for such a development the data presented does illustrate the importance of materials characterisation in terms of absorption and dispersion properties at mid-infrared frequencies and specifically in the region of 10.6 μm. Whereas materials based on

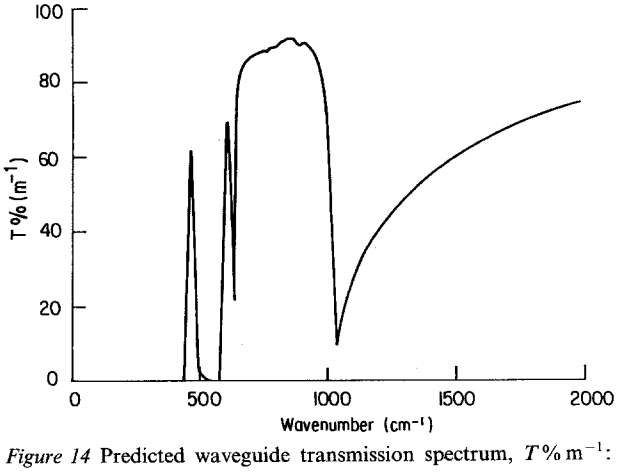

Figure 14 Predicted waveguide transmission spectrum, $T\%\,m^{-1}$: for hot pressed alumina, 99.9% Al_2O_3.

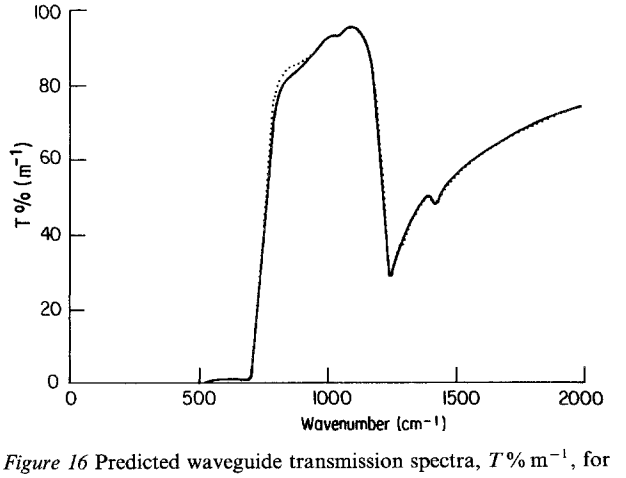

Figure 16 Predicted waveguide transmission spectra, $T\%\,m^{-1}$, for beryllia: (a) —BeO (1), (b) ···· BeO (2).

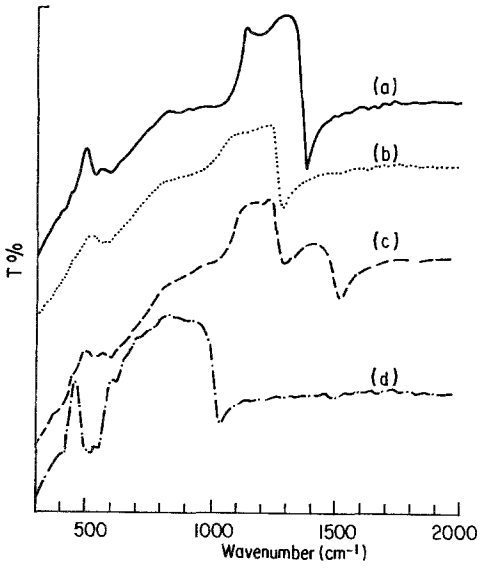

Figure 17 Measured transmission spectra, $T\%$, through small bore tubes: (a) fused silica, (b) soda-lime glass, (c) Pyrex, (d) recrystallized alumina.

glasses and glass–ceramics offer potential advantages in fabrication and flexibility, it is unlikely that the required absorption and dispersion at CO_2 lasing frequencies will be achieved with silica based glasses. Future work should be directed to those glass systems whose molecular vibrational transitions are displaced to longer wavelengths, and with particular attention to compositional refinements which minimize the refractive index and absorption coefficient at 10.6 μm.

Acknowledgements

Acknowledgements are due to Dr G. J. Hill for his encouragement and the provision of facilities, and to the board of ERA Technology Ltd for permission to publish this work.

References

1. E. GARMIRE, T. McMAHON and M. BASS, *Appl. Phys. Lett.* **29** (1976) 254.
2. *Idem, ibid.* **31** (1977) 92.
3. M. MIYAGI and S. KAWAKAMI, *J. Lightwave Technol.* **LT-2** (1984) 116.
4. M. MIYAGI, A. HONGO, Y. AIZAWA and S. KAWAKAMI, *Appl. Phys. Lett.* **43** (1983) 430.
5. T. HIDAKA, T. MORIKAWA and J. SHIMADA, *J. Appl. Phys.* **52** (1981) 4467.
6. T. HIDAKA, K. KUMADA, J. SHIMADA and T. MORIKAWA, *ibid.* **53** (1982) 5484.
7. Y. MIMURA and C. OTA, *Appl. Phys. Lett.* **40** (1982) 773.
8. T. J. BRIDGES, J. S. HASIAK and A. R. STRAND, *Opt. Lett.* **5** (1980) 85.
9. D. A. PINNOW, A. L. GENTILE, A. G. STANDLEE, A. J. TIMBER and L. M. HOBROCK, *Appl. Phys. Lett.* **33** (1978) 28.
10. S. SAKURAGI, M. SAITO, Y. KUBO, K. IMAGAWA, H. KOTANI, T. MORIKAWA and J. SHIMADA, *Opt. Lett.* **6** (1981) 629.
11. P. H. GASKELL and D. W. JOHNSON, *J. Non-Cryst. Solids* **20** (1976) 153.
12. F. J. J. CLARKE and J. A. LARKIN, Certificate of Measurement, National Physical Laboratory, Teddington, UK (1984).
13. A. S. BARKER, *Phys. Rev.* **132** (1963) 1474.
14. P. J. ZANZUCCHI, M. T. DUFFY and R. C. ALIG, *J. Electrochem. Soc.* **125** (1978) 299.
15. E. LOH, *Phys. Rev.* **166** (1968) 673.

Received 25 March
and accepted 2 April 1985